

Proceedings of International Workshop on Micro-Pattern Gas Detectors
pp. 119-123 (1999); pres. at Micro-Pattern Gas Detectors Workshop,
Orsay, France, 28-30 June (1999).

BNL 66497

Micro-Pin Array Detector (MIPA):
First Test Results*

P. Rehak, G. C. Smith, J. B. Warren, and B. Yu
Brookhaven National Laboratory, Upton, NY 11973

May, 1999

*Work supported by the U.S. Department of Energy: Contract No. DE-AC02-98CH10886.

Micro Pin Array Detector (MIPA): First Test Results

P. Rehak, G.C. Smith, J.B. Warren and B. Yu

Brookhaven National Laboratory, Upton, NY 11973, USA

Abstract

A novel gas proportional detector, consisting of an array of pins immersed into a cathode made out of closely packed hexagonals has been developed. The resulting geometry of the detector is 3 dimensional. Electron multiplication is limited to a region in close proximity to the tip of each pin, where the electric field decreases with distance from the pin at a rate faster than $1/r$, the rate that exists in a traditional wire chamber. The multiplication region is limited to a small part of the detector volume leading to stability of operation up to high charge gas gains.

The amplification region is located far enough from any dielectric surface that the gas gain is insensitive to the charge state of the surface, a significant benefit compared with many other micro-pattern detectors. The microscopic dimensions of the individual pins of the array result in signals whose total duration is about a microsecond. Two identical, but opposite polarity signals are detected, one on the pin and one on the cathode. Both signals can be used by two independent, charge division, read-out systems to obtain unambiguous x-y position information of the primary ionization.

Introduction

A novel gas amplifying micro-structure is being developed for use as a position sensitive X-ray detector for dynamic crystallography at the National Synchrotron Light Source (NSLS) at Brookhaven National Laboratory. The energy of the X-rays is about 10 keV, that is, within the energy region where several centimeters of xenon at atmospheric pressure are sufficient to fully absorb the scattered radiation. The detector should provide a high resolution image of the diffraction patterns with an effective number of pixels of at least 1 million with the same resolution in both x & y directions. This implies that the relative position resolution should be better than one part in a thousand in each direction. Furthermore the total rate on the detector can approach 100 MHz.

The linear position resolution of the detector should be slightly smaller than the photon beam size, which is about $300\mu\text{m}$ rms for NSLS crystallography beam lines. It is not easy to achieve these relative and absolute resolutions with such a high flux of incoming photons

with standard wire chamber technology.

Nevertheless, the recently published method of decreasing parallax error [1] makes a xenon gas detector a valuable candidate for dynamic crystallography. The use of some form of "Micro-Pattern" gas amplification may be a suitable approach to achieve the required specifications, particularly if the complete detector is fabricated from smaller independent segments.

This contribution is organized as follows. In the next section we will define the criteria for the stable operation of this type of the gas proportional detector. Then we will describe the geometry of the multiplication structure and of the full detector. We will finish by presenting a few results and conclusions.

Stability of the Gas Amplification

To achieve the required longterm, stable performance with a "Micro-Pattern" detector the amplification region should satisfy the following two conditions:

1. No dielectric surface near the avalanche region.
2. First order stability of the field in the avalanche region with respect to the electric run-away phenomena (discharge).

The importance of the first condition is well documented in the literature dealing with the instabilities in most of the Micro-Pattern Gas Detectors [2] and is easy to understand. The charge on the surface of a dielectric depends on the previous history of the electric field and charges in the region above the surface. The presence of the charges on the surface influences the electric field in the amplification region leading to well documented instabilities. Attempts to overcome this problem by using very high resistivity glasses or other layers have not been fully successful. [3]

We will elaborate in more detail on the second requirement of the stability of the amplification. In order to achieve the desirable gas gain in the amplification region a set of suitable voltages are applied on the electrode structures of the gas detector. In the absence of any space charges within the gas of the detector, the geometry of the amplification region and the applied voltages define completely the electric field within the avalanche region. The amplification of the electrons in this region filled with a given gas mixture at a given pressure depends only on the electric field. However, once the avalanche takes place, electrons are removed from this region much faster

This research was supported by the U.S. Department of Energy under Contract No. DE-AC02-98CH10886.

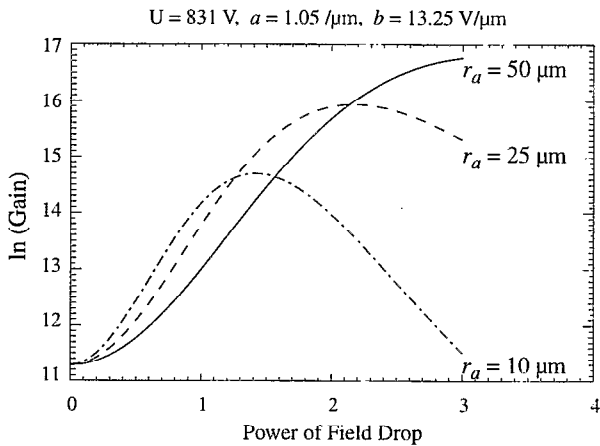


Figure 1: Natural logarithm of the gas gain as a function of the parameter n , called power of the field drop. The three curves correspond to different “anode radii” r_a . In all cases the radius of the cathode (extent of the field) is $r_c = r_a + 175 \mu\text{m}$.

than the positive ions. The presence of positive ions within the region modifies the electric field. If the modified electric field corresponds to a field with higher gain, electrons arriving in the avalanche region produce even more charge and the combined effect can lead to a run-away phenomenon or an electric discharge. The condition of “First order stability” requires that the applied field in the charge free amplification region corresponds to the maximum of the gas gain. Any deviation from this field due to the presence of space charge should decrease the gain and should prevent the amplification run-away.

Our analysis will model the gas amplification according to the classical work by Townsend. The avalanche process is described by the number of ionization collisions per unit length, called the first Townsend coefficient α . From this definition the natural logarithm of the gas gain is

$$\ln G = \int_{s_1}^{s_2} \alpha(U, U', s) ds, \quad (1)$$

where α can be a function of the voltage U and of the electric field $E = U'$ at a given point along the electron trajectory s . s_1 and s_2 are the first and the last points on the trajectory of electrons within the avalanche region respectively. We will moreover assume that the potential at the first and the last point of this region are U_1 and U_2 respectively. The second requirement on the stability is thus reduced to a variational problem of finding a function $U(s)$ that maximizes the gas gain in Eq.(1) with given values of voltages at both end points. ($U(s_1) = U_1$ and $U(s_2) = U_2$.)

The first Townsend coefficient α does not depend explicitly on the integration variable s and the Euler

equation

$$\frac{\partial \alpha}{\partial U} - \frac{d}{ds} \frac{\partial \alpha}{\partial U'} = 0 \quad (2)$$

gives the trivial solution $U' = (U_2 - U_1)/(s_2 - s_1) = \text{const}$. This is the case of a uniform field of planar geometry. However, for the values of α for our geometry the uniform field corresponds to the minimum rather than to the maximum of the gain.

To obtain the function $U(s)$ that maximizes gain, the class of functions $U(s)$ in Eq.(1) must be constrained to functions satisfying the conditions of the electrostatics. We will follow a less general approach searching for a field in a particular form

$$E(r) = \frac{E_a \cdot r_a^n}{r^n}, \quad (3)$$

where we write explicitly the magnitude of the electric field $E(r)$ rather than U' . The parameter n describes the form of the field. $n = 0$ corresponds to uniform field with 1 dimensional symmetry. $n = 1$ corresponds to the electric field around an anode wire with cylindrical symmetry. The formula is exact with r_a being the radius of the anode wire. $n = 2$ corresponds to a field having spherical symmetry. Other values of the parameter n have only a mathematical meaning.

We are planning to use a gas mixture of 80% Ar and 20% CO_2 . The first Townsend coefficient α at atmospheric pressure can be parameterized as

$$\alpha(E) = a \cdot \exp(-b/E), \quad (4)$$

where $a = 1.05/\mu\text{m}$ and $b = 13.25 \text{ V}/\mu\text{m}$. [4]

Fig. 1 shows results of Eq.(1) with electric field given by Eq.(3), α being defined in Eq.(4) for three different anode radii. We see that for practical values of the anode radius around $20 \mu\text{m}$ maximum gas gain is reached for $n \approx 1.7$. This power of the field drop is close to the power of the drop in the spherical geometry. A practical detector geometry generating such a field is that of a pin with a semi-spherical tip of radius r_a within a cylindrical cathode higher than the pin.

Simulations of the electric field in all three dimensions show that the electric field in a vertical line passing through the center of the pin decreases with distance as $r^{-1.88}$, at a line at 45° as $r^{-1.78}$ and even at any horizontal line passing through the center of the semi-sphere the decrease is $r^{-1.46}$.

Fig. 2 shows the scanning electron micrograph of the fabricated Micro Pin Array Detector (MIPA). The cathode consists of a 48×56 array of hexagonal cells in the xy plane. Each hexagon has a radius of $300 \mu\text{m}$ and a height of $400 \mu\text{m}$ in the z -direction. The wall thickness is $50 \mu\text{m}$. In the center of each hexagon, there is a cylindrical anode pin with the diameter of

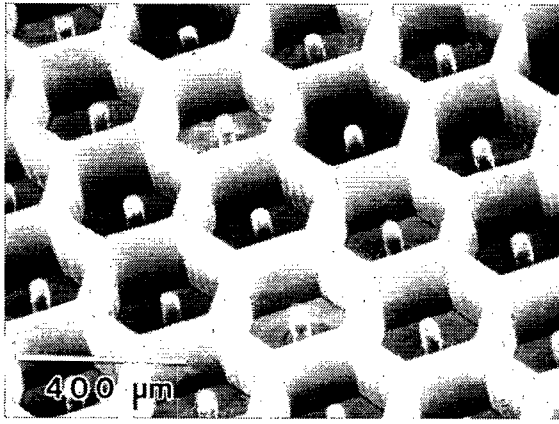


Figure 2: Electron microscope photo of the produced microstructure

50 μm and height about 200 μm . It may be helpful to visualize the MIPA geometry either as an extension of the microdot detector [5] into the third dimension, or as many individual pin detectors [6] compressed into a microscopic array using advanced lithographic techniques.

The position of the tip of the pins well below the upper plane of the cathode is the reason for the rapid change in electric field with the distance from the center of the anode tip. However, this depth may lead to a problem with full collection of signal electrons produced by the X-rays in a drift volume about a centimeter thick directly above the cathode. All negative lines of force starting from the thin window of the detector which encloses the drift volume from the above must end on anodes, none of them on the cathode. A deeper position of the anode tips inside the cathode structure requires a higher field in the amplification region relative to the field in the drift region. The chosen depth is a compromise between the sphericity of the amplification field, that is, the stability of the operation and full collection of the electrons with a reasonable value of the drift field. The hexagonal form of the individual cells minimizes the front surface of the cathode array as seen by signal electrons thus improving the collection properties of the array.

The MIPA was produced by sequential patterning of a UV-sensitive photoresist known as SU-8. This resist is quite transparent in the UV wavelength range used for exposure, and microstructures with aspect ratios as high as 18:1 can be patterned using a contact mask aligner. After UV exposure with an appropriate mask and annealing, the epoxy-based resist cross-links to form a rigid microstructure with good mechanical properties. Vacuum evaporation is used to metalize the surfaces of the anode and the cathode arrays. A small region at the bottom of the structure is left uncoated to provide the electrical insulation between anodes and cathodes.

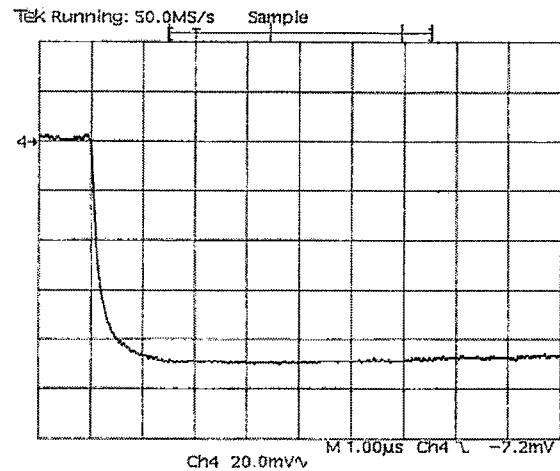


Figure 3: Signal waveform at the output of a charge sensing preamplifier connected to the cathode of the MIPA structure excited by a 5.9 keV X-ray.

Experimental Results

The MIPA structure was enclosed in a box with an entrance window at a distance of 1cm from the cathode. All anodes were connected together and also the cathode structure was left electrically undivided for these tests. The volume was filled with a mixture of 80% Ar and 20% CO_2 . The detector is usually operated with the cathode at ground potential, the anodes at a potential of about +600 Volts, with the entrance window at negative potential.

Fig. 3 shows a signal waveform at the output of a charge sensing preamplifier connected to the cathode of the MIPA structure excited by 5.9 keV X-rays. An identical but inverted waveform was observed from an amplifier connected to the anodes. We see that the rise time of the integrated pulse, that is, the duration of the current signal, is about 1 μs . This corresponds to the drift time of the positive ions traversing the distance between the tip of the anode and the top plane of the cathode array.

Fig. 4 shows X-rays spectra with a) only a small spot illuminated and b) with the entire detector illuminated. We believe that the worsening of the resolution for the full illumination of the detector is due to geometric imperfection of the array and we are working to improve it.

Fig. 5 shows the dependence of the gas gain measured with a charge sensing preamplifier followed by a 1 μs single delay line shaper on the anode voltage. The potential of the entrance window was held at -500 Volts. The detector can operate at a gain up to several times 10^4 without any discharges. The X-ray energy was 5.4 keV.

The gas gain dependence on the rate of incident X-rays has also been studied. Using uniform irradiation of

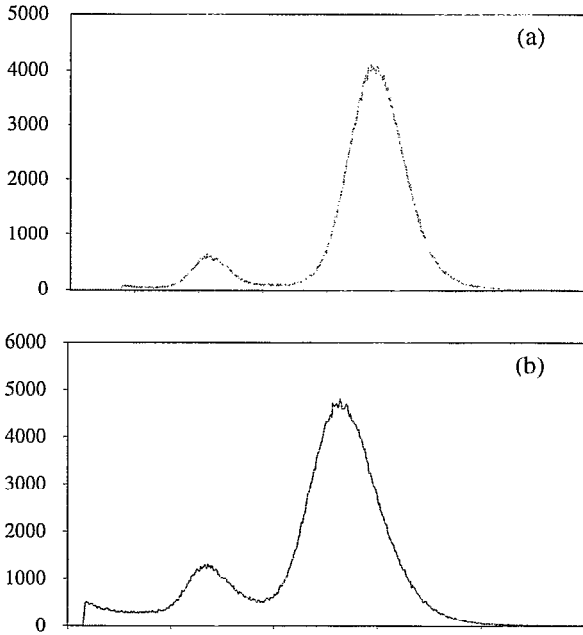


Figure 4: X-ray spectrum from MIPA detector. a) small area illuminated by 5.4 keV photons from an X-ray tube. b) entire prototype illuminated by 5.9 keV Mn fluorescence X-rays.

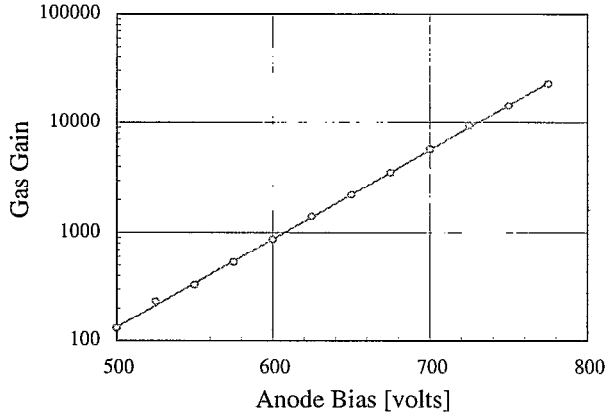


Figure 5: MIPA gas gain as a function of the anode pin bias voltage.

5.4 keV, a repeatable decrease in gain of about 10% for a rate of 10^6 X-rays $\text{mm}^{-2}\text{s}^{-1}$ was observed (not shown). This decrease may be due to the space charge, but it is an acceptable decrease for most of the applications.

The geometry and the electric field of the amplification region of the MIPA detector are such that not all the positive ions created by the avalanche process return back to the window. Fig. 6 shows the ratio of the current flowing to the entrance window, that is, traversing the whole drift distance of the detector and the current

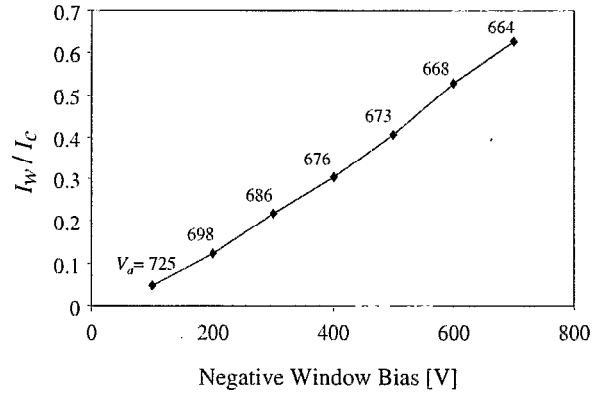


Figure 6: Ratio of current of positive ions returning to the entrance window and current of ions flowing into the cathode as a function of the drift field.

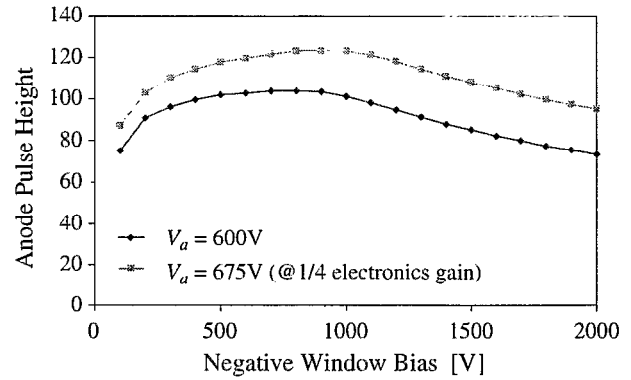


Figure 7: Pulse height of monochromatic X-rays as a function of the bias applied on the entrance window for two different anode voltages.

flowing to the cathode structure as a function of the negative voltage applied to the window. The anode voltage was also changed in a way to keep the gas gain constant. For small values of the drift field only about 5% of the positive ion created by avalanches are returning to the window traversing the drift region. The ratio increases almost linearly with the drift field. However, the drift time of positive ions within the drift volume decreases with the drift field. The combined effect is such that the density of the positive charges in the drift region of the detector is, in first order, independent of the drift field for the same flux of X-rays and the same gas gain.

Fig. 7 show the dependence of the pulse height of 5.9 keV X-ray peak on the negative drift voltage for two different values of the anode voltage. For values of negative window voltage smaller than about 700 V, that is, for the drift field below 700 V/cm the pulse height increases due to the increase of the electric field in the amplification region. However, a decrease in the pulse height is well visible once the negative voltage on the

window reaches 1000 V. Clearly, the gas gain cannot decrease with higher values of the electric field and our explanation is that a fraction of the primary electrons are being lost on the cathode structure of the MIPA. This hypothesis is supported by an observed worsening of the resolution for the higher value of the drift field and also agrees with the field simulation. We may increase the range of drift field values for full collection on primary electrons by producing structures having the anodes slightly higher relative to the top of the cathode structure.

Conclusions

The newly developed Micro Pin Array Detector seems to be a promising detector for uses extending beyond its main purpose as a X-ray detector for a time resolved crystallography.

Acknowledgements

The authors wish to thank E.F. Von Achen and D.C. Elliott for assistance in the detector assembly.

References

- [1] P. Rehak, G.C. Smith and B. Yu, "A Method for Reduction of Parallax Broadening in Gas-Based Position Sensitive Detectors", IEEE Trans. Nucl. Sci. 44 (1997) 651-655.
- [2] A. Bressan et al, "High Rate Behavior and Discharge Limits in Micro-Pattern Detectors." Nucl. Instr. and Meth. A424 (1999)321-342.
- [3] C. Richter, "Microstrip-Gas-Chambers for the HERA-B Experiment", This proceeding.
- [4] J.C. Armitage et al., "A Study of the Effect of Methane and Carbon Dioxide Concentration on Gas Amplification in Argon Based Gas Mixtures", Nucl. Instr. and Meth., A271 (1988) 588-596.
- [5] S.F. Biagi et al., "Further Experimental results of Gas Microdot Detectors", Nucl. Instr. and Meth., A392 (1997) 131-134.
- [6] J.E. Bateman, "The Pin Detector - a Simple, Robust, Cheap and Effective Nuclear Radiation Detector", Nucl. Instr. and Meth. A238 (1985) 524-532.